Environmental Science Nano

Accepted Manuscript

ROYAL SOCIETY OF CHEMISTRY

rsc.li/es-nano

Title: Induction of Micronuclei by Multi-Walled Carbon Nanotubes interacting with Humic Acids in cultured human lymphocytes

Maria-Sophia Vidali [1], Eleni Bletsa [2,3], Antonios Kouloumpis [3], Charalambos G. Skoutelis [1], Yiannis Deligiannakis [2], Dimitrios Gournis [3], Dimitris Vlastos [1]***

[1] Department of Environmental and Natural Resources Management, University of Patras, Seferi 2, Agrinio 30100, Greece

[2] Department of Physics, University of Ioannina,GR-45110 Ioannina, Greece

[3] Department of Materials Science and Engineering, University of Ioannina, GR-45110 Ioannina, Greece

***Corresponding author:**

Dimitris Vlastos

Department of Environmental and Natural Resources Management

University of Patras

Seferi 2, Agrinio 30100, Greece

TEL: +302641074148

E-mail address: dvlastos@upatras.gr

****Co-corresponding author:**

Yiannis Deligiannakis

E-mail address: ideligia@cc.uoi.gr

Keywords: genotoxicity; humic acids (HA); Humic-acid-like polycondensates (HALP); cytokinesis block micronucleus (CBMN) assay; multi-walled carbon nanotubes (MWCNTs)

Nano impact

A genotoxicity mechanism of multi walled carbon nanotubes (MWCNTs) interacting with Humic Acids (HA) is revealed. The interfacial properties of MWCNT-HA formations were characterized with ATR-FTIR, Atomic Force Microscopy and Dynamic Light Scattering. Using natural and synthetic/metal-free Humic polymers the mechanisms of colloidal dispersion are correlated with the revealed genotoxicity. Moreover the geno- *vs.* cytotoxicity phenomena are quantitatively distinguished. These phenomena originate from the action of Humic Macromolecules as "chaperons" that shuttle MWCNTs into the cell compartments.

Abstract

Mixtures of multi walled carbon nanotubes (MWCNTs) with natural humic acids (Leonardite humic acid, LHA) or humic acid-like polycondesates (HALP) were evaluated, for the first time, about their potential genotoxic and cytotoxic effect in cultured human lymphocytes. The genotoxic evaluation of the tested materials, either separately or in combination, for the detection of micronuclei (MN) in the cytoplasm of interphase cells, was performed by the cytokinesis block micronucleus (CBMN) assay. A comparative analysis of the genotoxicity and cytotoxicity reveals that in the tested concentrations [MWCNTs+LHA] mixture is more genotoxic and slightly more cytotoxic than the [MWCNTs+HALP] mixture. MN induction observed in human lymphocytes, demonstrates that humic substances enhance the genotoxic effects of MWCNTs. In addition, the present data highlight a -so far unforeseen- potential genotoxic effect as the result of both clastogenic and aneugenic action of the particular mixtures on human lymphocytes.

1 Introduction

Carbon nanotubes (CNTs) are fiber-shaped particles consisting of graphite hexagonal-mesh planes present as a single-layer (single-walled CNTs, SWCNTs) or as multilayers with nest accumulation (multi-walled CNTs, MWCNTs). Their potential applications are broad, e.g. in CNT-enhanced plastics, electromagnetic shielding, antistatic materials, flexible fibers and advanced polymers, medical/health fields, and scanning probe microscopy [1]. In 2005 the worldwide CNTs' production was ~0.2 kilotons (ktn). In 2011, this production increased by more than a factor of 10 and soared to about 4.6 ktn/yr [2].

Nonetheless, despite their already widespread use, there is increasing need for pertinent information on their implications in human health and the environment [3,4].

The main reason of concern about CNTs is related to their fibrous structure, which is similar to that of asbestos, and a high-aspect-ratio nanoparticle theory has already been suggested for CNT toxicity [5]. Accordingly, as in the case of asbestos, high-aspect-ratio MWCNTs are more toxic and potent to induce mesothelioma than low-aspect-ratio MWCNTs [5]. The carcinogenic effect of biopersistent fibers, such as asbestos, has also been associated with the local generation of reactive oxygen species and inflammatory reactions while genotoxic effects related to these phenomena may also be implicated [6].

The small size and high surface-to-volume ratio of CNTs could also affect interactions at the cellular level, leading to enhanced permeability through the cell membrane with a profound influence on cellular dynamics [7]. Therefore, it is essential to investigate the potential hazards of CNTs to humans and other biological systems not only at cellular but also at subcellular level i.e. on the genetic material for example. While existing literature data primarily focus on the potential cytotoxicity of CNTs, with conflicting results, the study on genotoxicity of CNTs is beginning to emerge as an important research area [8].

In the recent reviews by Toyokuni [9] and Saito et al. [10] it is stated that certain types of MWCNTs are as carcinogenic to mesothelial cells as asbestos fibers, and the cytotoxicity, inflammatogenicity and carcinogenicity of a specific given type of MWCNT are modulated by factors such as its diameter, length, rigidity and surface modification. In addition, distinguishing the mutagenicity and genotoxicity of CNTs remains a challenging research task; some studies judged CNTs to be mutagenic or genotoxic and others did not. The so-far published results vary i.e. depending on the cell-type even within the same study.

Nowadays, there is particular concern regarding possible genotoxic effect of nanomaterials, through their use and release into the environment, including soil, as well as their impact to the food chain and especially in humans [11]. Engineered Nanoscale Materials (ENMs) are already being used in agriculture as "nano-fertilizers" [12]. In addition, a recent study has shown that low doses of MWCNTs, in normal media, improving water absorption, plant biomass and the concentrations of the essential Ca, Fe nutrients, opening a potential for possible future commercial agricultural applications [13]. On the other hand, such use of nanomaterials may be of concern to human health e.g. humans, especially farmers, may become exposed as a result of MWCNTs contamination in soil and/or through the potential interactions between MWCNTs and soil components, such as humic acid (HA). In this context, the present study aimed to investigate the potential genotoxic effects of the MWCNTs in combination with the main soil component, such as soil organic matter, on humans.

More specifically, the potential of soil components i.e. humic acid (HA) macromolecules, in enhancing bioavailability of CNTs has to be carefully assessed. Due to their poor solubility and dispersability -in aqueous or polar solvents- MWCNTs are prone to aggregation and deposition in water due to strong inter-nanotube van der Waals forces [14,15].

Humic acids (HA), represent the most abundant fraction of humic substances, which are the most relevant chemically and biochemically reactive components of soil organic matter [16]. HA has been shown to be very efficient in enhancing water-dispersability of CNTs [14,15]. HA can be associated with the CNTs surface e.g. either *via* hydrophobic π-π interactions or/and by a physical wrapping of the HA macromolecules around CNTs. The high charge content of HA i.e. typically up to 1-4 meq/100 mg [17], makes the so-formed [HA+CNT] composite highly anionic at pH>4, and this results in their high dispersability in water. On the other hand, HAs are natural polyelectrolytes that regulate biological membranes' permeability [18,19]. This renders HA as potent cofactors able to shuttle exogenous entities e.g. such as nanomaterials, to cells' internal compartments. In this context herein the effect of contaminant presence of HA and CNTs on human cell-nucleus has been studied.

Two types of well characterized HAs were used: [i] a reference Leonardite HA (herein codenamed LHA) obtained from the International Humic Substances Society (IHSS), [ii] a well characterized, metal-free, synthetic Humic-Acid-Like-Polycondensate (HALP) produced from simple organic precursors with no use of co-catalsyst [20]. As demonstrated by Giannakopoulos et al. [20] HALP replicates the essential physicochemical parameters e.g. charge, structural carboxy/phenolic content, radicals, that are pertinent in the present study, however HALP is free of any adventitious ions -in particularly Fe- that might be involved in adverse oxidative-stress events.

The aim of the present work was to study the potential genotoxic effects of MWCNTs in combination with LHA or HALP in human lymphocytes *in vitro*. In general, the genotoxicity is directly linked to the mutagenic and carcinogenic effects of chemicals. To cover the whole spectrum of the genetic damage that can occur, usually they are used a combination of assays both *in vitro* and *in vivo* conditions. For this purpose the widely used cytokinesis block micronucleus (CBMN) assay in human lymphocyte cultures, which is a sensitive indicator of

chromosome structural and numerical changes, was selected and used herein i.e. as a validated method accepted for regulatory purposes [21-23].

Micronuclei (MN) may originate from acentric chromosome fragments or whole chromosomes that are unable to migrate to the poles during the anaphase stage of cell division. The simplicity, rapidity and sensitivity of the CBMN assay make it a valuable tool for genotoxicity screening [23].

Overall, the main objectives of the present study were: [a] to evaluate the genotoxic and cytotoxic effect of MWCNT interacting with LHA and HALP, in human lymphocytes *in vitro*, [b] to understand the physical mechanism of the observed genotoxicity and cytotoxicity in relation to the enhanced water solubility of the LHA+MWCNTs, HALP+MWCNTS.

2 Method

2.1 Synthesis of HALP

HALP was produced by the oxidative polymerization of gallic acid and protocatechuic acid in molar ratio 1:1 according to Giannakopoulos et al. [20] with no use of a cocatalyst. The procedure is described in the Supplementary information (SI). The so obtained free-of-metals HALP was fully characterized as detailed by Giannakopoulos et al. [20].

2.2 Materials

MWCNTs (6-9 nm diameter, 5 μm length) with >95% purity were supplied by Sigma–Aldrich (CAS No. 724769) and purified in a metal-free form according to Georgakilas et al. [24]. Leonardite HumicAcid standard (LHAS04) was purchased from the IHSS and used with no further purification.

2.3 HA Stock solutions

Stock solutions (500 mg/L) of the LHA and HALP were prepared with Milli-Q water (Millipore-Acedemic system) and their desired pH was adjusted with small volumes of NaOH and HNO_3.

2.4 MWCNT-HA suspensions

The stock suspensions MWCNTs and HAs [LHA or HALP] were prepared as follows: (a) 55 mg of MWCNTs was dispersed in 100 ml deionized/ultrapure water (b) 220 mg of LHA was dispersed in 100 ml deionized/ultrapure water and (c) 88 mg of HALP was dissolved in 100 ml deionized/ultrapure water. From the stock solutions, appropriate volumes -which correspond to the final concentrations of the tested mixtures- were added in our cultures. The solutions were sonicated using low-power sonication. More particularly based on the Dynamic Light Scattering data, detailed in the following, we have applied a total of 0.6 kJ power per ml of solution. Typically this is achieved by applying 50 Watt sonication power for 20 minutes per 10 ml volume. This can be routinely performed using a commercial bath sonicator. Mild/low-power sonication protocol results in no physical damage of MWCNTs thus excluding any artificial generation of edge-related radical species that might generate reactive oxygen species. The dispersionwas then left under stirring overnight. Water was the only solvent employed, and no organic solvents were used.

2.5 Materials' Characterization

2.5.1 Attenuated Total Reflection (ATR)-FTIR

ATR-FTIR spectra was recorded on a Shimadzu FT-IR 8400 infrared spectrometer Perkin Elmer Spectrum-GX in the region of 800–3000 cm^{-1} using a (ZnSe)-attenuated total reflection accessory. Each spectrum was the average of 300 scans collected at 2 cm^{-1} resolution. Zn-Se crystal permitted the study of aqueous samples at pH range 4-9.

2.5.2 Atomic Force Microscopy (AFM)

AFM images were obtained in tapping mode with a 3D Multimode Nanoscope, using Tap-300G silicon cantilevels with a tip radius <10 nm and a force constant of ≈20–75 N m-1. Samples were deposited onto silicon wafers (P/Bor, single side polished) from aqueous dispersions by drop -casting. At least 40 AFM images were analyzed in each sample. In the case of the HA/CNT samples the occurrence of the single/unbundled CNTs was 85-90% of the studied images.

2.5.3 Dynamic Light Scattering (DLS) preparation and measurement

To determine the particle size of MWCNTs in suspension, we have investigated in detail the effect of sonication energy on the dispersion/size of the CNTs'. The total ultrasound energy delivered per ml of solution is calculated as:

Total ultrasound Energy delivered per ml= [Ultrasound Power (Watts) x Sonication Time] / Solution Volume (ml)

We have screened sonication energies from low (0.2 kJ/ml) up to high (8 kJ/ml). Low sonication energies (0.2-0.6 kJ/ml) were produced using a common path sonicator (Pranson 2000, 50 Watt) i.e. varying the sonication time. A full [energy per ml] scale (0.2 to 8 kJ/ml) was investigated using a probe sonicator Sonic V500 delivering a maximum of 500 Watts. DLS data show that for the same energy per ml the method of sonication e.g. bath or probe, gives the same DLS results. Thus controlling the total energy per ml allows a precise parametrisation of the sonication protocol i.e. instead of varying only the sonication time or only the power.

In the present experiments we have studied suspensions of 10 mg/L i.e. 10 μg/ml MWCNTs in various media [1] only H_2O, pH 6.5, [2] the culture medium, pH 6.5 [6.5 ml Ham's F-10 medium (Gibco), 1.5 ml foetal bovine serum (Gibco) and 0.3 ml phytohaemagglutinin (Gibco)]. The effect of HALP was studied by adding 10 mg/L of HALP in the suspension of the MWCNTs.

In all cases the agglomerate size in solution was determined by DLS at short incubation times [30 minutes] as well as after 72 hours i.e. conditions similar to the biological cultures. Dynamic Light Scattering (DLS), Malvern Zetasizer, model Nano ZS, measurements were performed in quartz cuvettes.

2.6 CBMN assay in human lymphocytes in vitro

Blood samples were obtained from two non-smokers, healthy individuals (21 and 25 years old) not undergoing any drug treatment, free of viral infection or X-ray exposure in the recent past. Blood samples were kept under sterile conditions in heparinized tubes. Whole blood (0.5 ml) was added to 6.5 ml Ham's F-10 medium (Gibco), 1.5 ml foetal bovine serum (Gibco) and 0.3 ml phytohaemagglutinin (Gibco) to stimulate cell division. The effect of MWCNTs, LHA and their mixture were studied at three different concentrations (5, 15, 25 μg/ml), (20, 60, 100 μg/ml) and (5+20, 15+60, 25+100 μg/ml) respectively. The reported results in Table 1 represent the pooled data from the two donors' replicated cultures [25]. Furthermore, the effect of MWCNTs, HALP and their mixture were studied at four different concentrations (5, 15, 25, 30 μg/ml), (8, 25, 42, 50 μg/ml) and (5+8, 15+25, 25+42, 30+50 μg/ml) respectively. The reported results in Table 2 represent the pooled data from two independent experiments. Mitomycin-C (MMC) (Sigma) at final concentration of 0.05 μg/ml served as positive control. 44 h after initiating cultures, 6 μg/ml Cytochalasin-B (Cyt-B) (Sigma) was added to the culture medium to block cell division. The use of cytochalasin-B, an inhibitor of actin polymerization, which prevents cytokinesis while permitting nuclear division leads to formation of binucleated (BN) cells which are scored for the presence of MN [23].

Cultures were incubated at 37^{o}C in a humidified atmosphere of 5% CO_2 for 72 h. The procedure for slide preparation is described in the SI section. Standard criteria were used for scoring MN [26].

To determine possible cytotoxic effects, the Cytokinesis Block Proliferation Index (CBPI) was calculated by counting at least 2000 cells for each experimental point. CBPI is given by the equation:

$$CBPI = [M_1 + 2\ M_2 + 3(M_3 + M_4)]/N$$

where M_1, M_2, M_3 and M_4 correspond to the numbers of cells with one, two, three and four nuclei and N is the total number of cells [23].

The calculation of MN size was also used as an additional parameter to assess the activity of the tested substances as clastogenic or aneugenic [27,28]. MN size is expressed as the ratio MN_d/CN_d (MN_d=MN diameter/CN_d=cell nucleus diameter).

MN size was characterized as "small", when $MN_d/CN_d \leq 1/10$, "medium" for MN_d/CN_d=1/3 to 1/9 and "large" for $MN_d/CN_d \approx 1/3$ [27].

Small size MN are more likely to contain acentric chromosome fragments indicating a clastogenic effect, while large size MN may possibly contain whole chromosomes thus indicating an aneugenic effect [27,28].

2.7 Statistical analysis

All results are expressed as the mean frequency ± standard error (MF ± se). The statistical analysis of the MN data was conducted using the *G*-test for independence on 2x2 tables. The chi-square test (χ^2 *test)* was used for the analysis of CBPI among each treatment. Statistical decisions were based on a significance level of 0.05. The statistical software used for data analysis was the Statistical Package for Social Sciences (SPSS) for Windows, version 17.0.

3 Results

3.1 Dispersion Effect of HAs on MWCNTs - Dynamic Light Scattering (DLS)

The sample-pictures in Figure 1 exemplify the dispersability difference between MWCNTs in H_2O in the absence of HAs (Figure 1a), and in the presence of HAs (Figure 1c). In the

absence of HAs, negligible dispersion of MWCNTs was detected even after 8 kJ/ml of sonication (Figure 1a). In the presence of HAs, under low-energy sonication 0.6 kJ/ml, MWCNTs form a non-precipitating suspension which remained practically unaltered for at least two weeks, as illustrated in Figure 1c and this is an indication that HAs solubilizes the MWCNTs. Complete solubilization of the MWCNTs in the presence of HAs, was achieved under 0.6 kJ/ml sonication energy, as illustrated in Figures 1d and 1e, for HALP and LHA respectively. We notice a color difference after complete solubilization of the MWCNTs between HALP (grey) and LHA (more brown) in comparison with the HALP (Figure 1b). These colorimetric observations can be explained using DLS that gives quantitative information on the debundling/disaggregation process. Herein we discuss the DLS data for 10 μg/ml of MWCNTs that is within the range i.e. 5-30 μg/ml, studied in cell cultures, described hereafter. Analogous DLS experiments for higher MWCNT concentrations (25 μg/ml) show increasing agglomeration (data not shown).

DLS for MWCNTs/HA in H_2O: In Figure 2a, in the absence of HALP, 10 μg/ml of MWCNTs suspension in H_2O showed strong aggregation with average hydrodynamic particle diameter 1700-1800 nm (Figure 2a blue line). This hydrodynamic size did not change even after 8 kJ/ml sonication energy (data not shown). This is a direct manifestation of the –well known- strong aggregation of MWCNTs, that is in agreement with the visual observation of the heterogeneous suspension that forms the black precipitates in Figure 1a. In the presence of HALP (Figure 2a, red line) the DLS diameter was decreased to 180-190 nm with just 0.6 kJ/ml energy. Higher ultrasonic energy resulted in a slow decrease of the DLS size, leveling down to 160 nm for energy 1.2 kJ/ml or higher (not shown).

DLS for MWCNTs/HA in the Cell- Culture medium: When dispersed in the culture medium 10 μg/ml of MWCNTs, showed a main fraction (>80%) with low DLS diameter 200-220 nm, in the absence of HALP (Figure 2b, blue line). A lower fraction (<20%) was highly

aggregated i.e. it retained its bundled 1700-1800 nm state. Higher ultrasonic energy i.e. up to 2 kJ/ml did not decrease these DLS sizes. Thus DLS data reveal that the cell-culture medium itself has the ability to cause debundling in a significant fraction of the MWCNTs. This is attributed to the proteins that constitute this culture medium. In the presence of HALP (Figure 2b, red line) in the culture medium, the DLS size was decreased to 140-160 nm with 0.6 kJ/ml energy, with no further decrease at higher ultrasonic energies. After 72h at rest in the culture medium, the MWCNT/HALP showed a fractional increase in the DLS size i.e. part of the particles formed aggregates of 180-200 nm, however the major fraction remained unaltered.

Overall, the DLS results show that both in H_2O as well as in the cell culture medium HALP macromolecules strongly debundle MWCNTs. The cell culture medium also debundles MWCNTs to some extent. The basis of the debundling effect of HALP is that HALP macromolecules, when associated on the CNT surface can decrease the stacking energy between the bundled CNTs, by introducing hydrophilic interactions via their charged groups. This is in agreement with Ghosh et al. [29] who have demonstrated that natural Humics enhance the colloidal stability/dispersion of nanotubes and other nanomaterials. Herein this effect was further investigated in detail for the HALP/MWCNT system using ATR-FTIR spectroscopy.

3.2 Interactions of MWCNTs-HALP and MWCNTs-LHA studied by ATR-FTIR spectroscopy

ATR- FTIR spectroscopy is a useful technique for the analysis of organic species adsorbed in the solid-solution interface [30]. Although the infrared spectra of pristine MWCNTs are featureless, FTIR spectroscopy using the ATR accessory is very informative for studying the functional groups attached to the sidewalls of the MWCNTs [30,31]. The ATR-FTIR spectra for MWCNTs interacting with HALP or LHA are presented in Figure 3. The pH-dependent

features in the ATR-FTIR spectra for the $MWCNT_S$-HA interactions were studied at different pH (e.g. pH 8.5, pH 6.5 and 5.0).

The ATR- FTIR spectra for HALP (black line) in Figure 3a show peaks in 1690-1750 cm^{-1} corresponding to C=O($v_{C=O}$) carboxyl stretches [31]. The peaks in 1400- 1650 cm^{-1} correspond to asymmetric stretching frequencies for aqueous carboxylates while those corresponding to the symmetric stretch are detected in 1300-1420 cm^{-1}. Signals at 1400-1600 cm^{-1} are assigned to phenyl ring stretches [20]. The band at 1155 cm^{-1} is ascribed to C-O stretches or O-H deformations of the C-OH groups [31].The ATR- FTIR spectra for LHA (black line) in Figure 3b show the same features as for HALP, however with inferior resolution of the spectral lines. This is attributed to the less-homogeneous structure of LHA *vs*. HALP. Upon interaction of MWCNTs with HALP and LHA severe changes are observed in the ATR-FTIR spectra (red lines in Figure 3 a, b). The interaction of MWCNTs with HALP affects the carboxylate peaks which are significantly diminished in the presence of MWCNTs. Moreover, the carboxylate vibrations at 1622 cm^{-1} shift to 1634 cm^{-1}. Thus the ATR-FTIR spectra provide direct evidence of strong interaction of the MWCNTs with the carboxylates of HALP or LHA. The carbonyl band at 1720 cm^{-1} disappeared, indicating specific interaction between MWCNTs and the carbonyl O.

The ATR-FTIR spectrum of MWCNTS-LHA is similar to that of MWCNTS-HALP (Figure 3b). More specifically, in LHA the peak at 1643 cm^{-1} is replaced by two peaks shifted to higher wavenumber (by Δv~5-10 cm^{-1}) indicative of MWCNTs interactions with carbonyl-O groups. The enhanced peak at ~1056 cm^{-1} is due to C-O stretches. Various previous studies have provided evidence that carboxyls of HA -as well as phenolic and aromatics- are strongly interacting with CNTs [15,32]. Overall, the present data in accordance with literature, are consistent with a structural picture where COO, R-OH groups of HALP and LHA interact with the sidewalls of MWCNTs, forming a stable embodiment [HA+MWCNT]. This

[HA+MWCNT] embodiment bears pH-dependent charge i.e. due to the chargeable carboxy/phenolics of HAs [14,15] and this determines the observed significant effect of pH on the debundling and solubilization of MWCNTs.

3.3 Atomic Force Microscopy (AFM)

AFM images of MWCNTs and MWCNTs+HALP, deposited on Si-wafer (Figure 4) allow a comparison of the morphological features of MWCNTs at the nano-scale, before (Figure 4a) and after (Figure 4b) the interaction with the HAs, in aqueous solution. A typical AFM image of MWCNTs in the absence of HA (Figure 4a) shows the aggregated structure of MWCNTs, i.e. despite the sonication treatment MWCNTS retain a bundled/aggregated form, in agreement with the DLS data. In the HALP+MWCNTs, well dispersed nanotubes are easily observed which obtain a mono-disperse structure (Figure 4b) with an average diameter 13-14 nm. As seen in Figure 4b the configuration of these MWCNTs might be twisted/curled, i.e. not an ideal straight-line shaped tube. The effective diameter of this conformation corresponds to the hydrodynamic diameter detected by DLS.

Overall, according to AFM images and DLS data the dispersions of MWCNTs in H_2O form aggregates, which in the presence of HAs "debundle", even under low-power sonication, forming monodispersed CNTs in 85-90% of the studied AFM images.

3.5 Genotoxic and cytotoxic effects by MWCNTs, LHA and their mixture

The results obtained from human peripheral blood lymphocyte cultures treated with different concentrations of MWCNTs, LHA, their mixture and MMC are shown in Table 1. The data in Table 1 reveal that MWCNTs or LHA, each one separately, were able to induce a minor increase in MN frequencies at all tested concentrations, *vs.* the control. MWCNTs induced a statistically significant increase ($p<0.01$ and $p<0.05$) on MN frequencies at concentrations 5 and 15 μg/ml respectively. In the case of mixed [MWCNTs+LHA] treatments our results showed a remarkable three to five-fold increase in MN frequencies *vs*. the control. More

specifically, MWCNTs+LHA induced statistically significant differences ($p< 0.001$) on MN frequencies *vs*. the control.

The cytotoxic effect was evaluated *via* the determination of CBPI for MWCNTs, LHA and their mixture. Regarding the cytotoxic index in all tested concentrations, no statistically significant differences were observed between control and treated cultures. The negative (5.25±0.48‰) and positive (54.75±4.13‰) control frequencies of MN found in our experiments are in accordance to the published values in the used assay [33].

The MN_d/CN_d size ratio of MN in the *in vitro* CBMN assay is an alerting index i.e. as effective as the Fluorescence i*n situ* Hybridization (FISH) analysis, for the discrimination of clastogenic and aneugenic effects [27,28,34-36].

Here, data on the MN_d/CN_d size ratio of MN (‰) induced by MWCNTs and their mixtures with LHA are presented in SI (Figure S1). A statistically significant increase in both small- and large-size MN frequencies was observed in all tested mixtures, except for the case of the large size MN in the MWCNTs+LHA (5+20 μg/ml) treatment. Moreover, statistically significant increase in large-size MN frequencies was observed in the MWCNTs-treatment (15 μg/ml).

3.6 Genotoxic and cytotoxic effects by MWCNTs, HALP and their mixture

The results shown in Table 2, reveal that there are no statistically significant differences between control and MWCNTs -or HALP- treated cultures. In the case of mixed MWCNTs+HALP treatments an approximately three-fold increase in MN frequencies *vs*. the control was found. MWCNTs+HALP mixtures induced a statistically significant increase ($p<0.001$) on MN frequencies at all tested concentrations *vs*. the control.

Regarding the CBPI index, to evaluate the cytotoxic effect, no statistically significant differences were observed between control and [MWCNTs/HALP and their mixtures] treated

cultures. The reported negative (5.0±0.0‰) and positive (57.0±6.0‰) control frequencies of MN in our experiments are in accordance to published values in a similar assay [33].

Regarding the MN_d/CN_d size ratio of MN (‰) induced by MWCNTs e.g. separately or in combination with HALP, there was a significant increase in both small- and large-size MN frequencies at the higher tested concentrations of MWCNTs+HALP mixtures (25+42, 30+50 μg/ml respectively). In the cases of lower concentrations of MWCNTs+HALP mixtures, statistically significant increase was observed in small (5+8 μg/ml) and in large (15+25 μg/ml) size MN frequencies, respectively (see SI, Figure S2).

4 Discussion

4.1 Significant enhancement of the genotoxic effect by MWCNTs+HA.

The present data reveal that natural HA (LHA) resulted in more severe MN enhancement than the synthetic HALP. Since the structural characteristics of HALP are similar to that of LHA, the additional MN increase can be attributed to adverse effects of heteroatoms, most likely Fe [16], present in natural LHA.

Previous studies on the genotoxicity of MWCNTs have been reported, however for much higher concentrations [37] than those used herein. The statistically significant genotoxic induction at MWCNTs concentrations of 5 and 15 μg/ml as well as the increased MN frequency at 25 μg/ml (Table 1), corroborate previous reports with regard to the genotoxic action of CNTs. More precisely, Lindberg et al. [38], examined the potential genotoxic effects of carbon nanotubes (CNTs; >50% single-walled, ~40% other CNTs) in cultured human bronchial epithelial cells (BEAS 2B) for 24, 48 and 72 hrs with various doses (3.8–380 μg/ml), using the single cell gel electrophoresis (comet) assay and the micronucleus (MN) assay. In the comet assay, CNTs induced a dose-dependent increase in DNA damage at

all treatment times, with a statistically significant effect starting at the lowest dose tested. In the MN assay, no increase in MN frequencies was observed with CNTs after the 24-h and 72-h treatment. The 48-h treatment caused a significant increase in MN frequencies at three doses (lowest 38 μg/ml) of CNTs. No dose-dependent effects were seen in the MN assay.

Similarly, Ghosh et al. [39] demonstrated the genotoxic effect of MWCNTs, using -among others- the comet assay in human lymphocytes. Significant genotoxic response was observed at the concentration of 2 μg/ml, followed by a gradual decrease at the higher concentrations tested and that may be due to the formation of crosslinks or the agglomeration of MWCNTs [39]. The findings of this study [39] are consistent with our present results with regard to the genotoxic induction observed in MWCNTs at the concentrations of 5 and 15 μg/ml, but not at the higher concentration of 25 μg/ml (Table 1). Taking into account the DLS data, we suggest that the observed decrease at the higher concentrations may be due to formation or agglomeration of MWCNTs, thus inhibiting their genotoxic action.

A recent study of Tavares et al. [40] evaluated, among others, the potential genotoxic effects of six different types of MWCNTs using the CBMN assay on human lymphocytes and clearly indicated MN induction, without dose-effect relationship, in the case two of the six MWCNTs examined. As commented by Tavares et al. [40] the observed differences in genotoxicity among closely related MWCNTs which may not be explained by the morphology and size of MWCNTs but rather by the agglomeration process in correlation with the tested concentrations.

Our results, on the negative genotoxic responses of HAs (Tables 1, 2) are supported by the research of Ferrara et al. [41], who applied the MN assay in human lymphoblastoid cell line (TK6) in order to evaluate the genotoxicity of HAs. The findings reported by Ferrara et al. [41], revealed the absence of genotoxic effect of the examined HAs samples .

In order to further assess the mechanism of genotoxicity action of MWCNTs and their mixtures with LHA and HALP we analyzed the size-distribution of induced MN. In general, the tested mixtures that induce MN may do so because they induce chromosome breakage (clastogenic effect), chromosome loss (aneugenic effect), or a combination of the two. The MN size ratio in the CBMN assay is an alerting index i.e. as effective as the Fluorescence *in situ* Hybridization (FISH) analysis for the discrimination of clastogenic and aneugenic effects [27,28,34-36]. As can be seen in SI (Figures S1 and S2), the tested mixtures of MWCNTs with HA or HALP induced a statistically significant increase in both small- and large-size MN. According to the latter, the large MN observed in MWCNTs and their mixtures with LHA and HALP-treated lymphocytes, might contain whole chromosomes, thus revealing an evidence of tested mixtures aneugenic potency, while the presence of small MN is more likely to contain acentric chromosome fragments indicating its clastogenic effect. This shows that the genotoxicity of MWCNT-HA is the result of clastogenic as well as aneugenic events. This observation, is corroborated by the study of Cveticanin et al. [42], which connects the formation of MN in human lymphocytes with the clastogenic as well as aneugenic activity of MWCNTs. Also, previous studies in human epithelial cell line (MCF-7) suggested that MWCNTs can induce MN by both clastogenic and aneugenic mechanisms [43].

4.2 Absence of cytotoxic effect

The CBPI index showed no statistically significant differences of the CBPI values which were observed between control and either MWCNTs or MWCNTs+HA treated cultures. Our results are in accordance with the recent findings of Tavares et al. [40] which found that CBPI was not significantly affected by any of the six different examined MWCNTs.

Kihara et al., demonstrated that HA from Indonesia induced cytotoxicity at concentrations greater than 50 μg/ml on human vascular endothelial cells [44]. Our observations on the cytotoxicity pattern of the tested HA (IHSS standard LHA and synthetic HALP) indicate that

they are not cytotoxic at all tested concentrations in cultured human lymphocytes. The observed differences in cytotoxicity pattern of the present tested HAs vs. that of Kihara et al. [44], could be attributed in their different physicochemical characteristics e.g. metal content, or structural profile of the macromolecules, which reflect the differences from one ecosystem type to another.

The concentrations of MWCNTs used in the present study are comparable to the concentrations used in several other studies. Lacerda et al. injected 300 μg MWCNTs per rat, which translates to a concentration of 20 μg/ml (average rat blood volume 15 ml and 200 g body weight) [45]. Deng et al. injected 10 μg MWCNTs per mouse, which translates to a concentration of 10 μg/ml (average mouse blood volume 1 ml and 20 g body weight) [46]. These animal imaging studies investigated the systemic administration of functionalized and radiolabeled MWCNTs. Recent studies on human cells, investigated the effects of MWCNTs on human microvascular endothelial cells at afinal concentration of 2.5 μg/ml [47] as well as on human lymphocytes at final treatment concentrations of 1 up to 10 μg/ml [39] and of 1 up to 300 μg/ml [40].

Our rationale for the selection of the, low, MWCNTs concentrations is also supported from a very recent study which investigated the application of nano-biotechnology to crop-science/agriculture and established the term "nanoagriculture" as a recent development. Tiwari et al. demonstrated that pristine MWCNTs at low concentrations (20 mg/l) benefit the growth of maize seedlings by enhancing water, nutrient transport and biomass [13]. These findings suggest a potential for the utilization of CNTs for optimizing water transport in arid-zone agriculture and of improving crop biomass yields.

4.3 A Physicochemical Mechanism

Our ATR- FTIR study shows that HA solubilizes the MWCNT *via* specific interactions of the COO groups with the CNTs surface. DLS provides quantitative data on "debundling" of

nanotube aggregates, in the presence of HALP. This observation correlates with the observed three to five-fold increase MN-induction by MWCNTs+LHA and MWCNTs+HALP. The straightforward implication of these data is that the formed LHA/HALP-MWCNTs embodiments have the potential to penetrate not only the cell membrane but also the nucleus membrane, inducing MN. Here is it of pertinence to notice that despite the partial debundling effect of the cell-culture medium i.e. in the absence of HALP, this is not enough to trigger the MN formation. On the other hand HALP appears to play critical role in MWCNTs' debundling and MN induction. This reveals that HALP has a multiple effect i.e. that is effectively shuttling MWCNTs into the nucleus, in addition to the debundling effect in solution.

Despite the fact that the cellular uptake of CNTs and its underlying mechanisms remain largely unclear [10] it is tempting to comment that associations of CNTs with specific proteins may alter their pharmacokinetic and pharmacodynamics behavior [48] as well as their genotoxic and/or cytotoxic activity [49]. In simulated cell culture conditions, MWCNTs are found to bind the highest number of proteins (133) compared to unmodified nanotubes (<100), suggesting covalent binding to protein amines [48]. In addition, Pacurari et al. demonstrated that MWCNT lead to an increase in cell permeability in human microvascular endothelial cells [47]. A recent report suggested that exposure to electromagnetic waves promotes CNTs entry not only into the cytoplasm of cells, but also into the nucleus [50].

Our present findings suggest a similarity between the mode of action of Humic macromolecules with analogous bio-macromolecules/proteins. The macromolecule acts as shuttle-like agent to enhance the permeability of [CNT/organic] into the internal cellular compartments. Her we provide the first evidence that via this mechanism, environmental factors –Humics- combined with CNTs, may induce direct genotoxic effects.

5 Conclusion

The present study revealed a statistically significant induction of MN frequencies in cultured human lymphocytes treated with a mixtures of MWCNTs+HAs. A comparative analysis of the genotoxicity and cytotoxicity in the tested concentrations reveals that the MWCNTs+LHA mixture is more genotoxic and slightly more cytotoxic than the MWCNTs+HALP mixture. The MN induction observed herein in human lymphocytes, reveals the ability of [MWCNTs+LHA or HALP] mixtures to enhance genotoxic effects, while there was a first evidence of the potential genotoxic effects as the result of both clastogenic and aneugenic action of the particular mixtures on human lymphocytes.

Taking into account that the examined concentrations were low, MWCNTs should be handled with great care, in order to minimize its environmental and human risk. From that point of view, their potential impact to the environment, the organisms and human health must be further investigated and confirmed.

Ethics Statement

The study was approved by the Ethics Committee of the University of Patras. After informed consent two healthy, non-smoking, males (20 and 25 years old) were used as blood donors to establish whole blood lymphocyte cultures. According to the donors' declarations, they had not been exposed to radiation, drug treatment or any viral infection in the recent past.

Declaration of interest

The authors report no conflicts of interest.

References

1. M. Ema, T. Imamura, H. Suzuki, N. Kobayashi, M. Naya and J. Nakanishi, *Regul. Toxicol. Pharm.*, 2012, **63**, 188–195.

2. M. F. L. De Volder, S. H. Tawfick, R. H. Baughman and A. J. Hart, *Science*, 2013, **339**, 535-39.
3. L. Braydich-Stolle, S. Hussain, J. J. Schlager and M. C. Hofmann, *Toxicol Sci.*, 2011, **88**,412–19.
4. S. M. Hussain, K. L. Hess, J. M. Gearhart, K. T. Geiss and J. J. Schlager, *Toxicol. In Vitro*, 2005, **19**, 975–83.
5. IARC, Monographs on the evaluation of carcinogenic risk to chemicals on man, Asbestos. 1977, **14**, 1–106.
6. J. S. Kim, K. Lee, Y. H. Lee, H. S. Cho, K. H. Kim, K. H. Choi, S. H. Lee, K. S. Song, C. S. Kang and I. J. Yu, *Arch. Toxicol.*, 2011, **85**, 775–86.
7. R. H. Hurt, M. Monthioux and A. Kane, *Carbon*, 2006, **44**, 1028–33.
8. A. M. Schrand, J. Johnson, L. Dai, S. M. Hussain, J. J. Schlager, L. Zhu, Y. Hong and E. Osawa, in *Safety of Nanoparticles, Nanostructure Science and Technology*, ed. T. J. Webster, Springer Science+Business Media, New York, 2009, ch. 8, pp. 159-187.
9. S. Toyokuni, *Adv. Drug Deliver. Rev.*, 2013, **65**, 2098–110.
10. N. Saito, H. Haniu, Y. Usui, K. Aoki, K. Hara, S. Takanashi, M. Shimizu, N. Narita, M. Okamoto, S. Kobayashi, H. Nomura, H. Kato, N. Nishimura, S. Taruta and M. Endo, *Chem. Rev.*, 2014, **114**, 6040−79 and references therein.
11. UWE (University of the West of England), Science Communication Unit, Bristol, 2013, Science for Environment Policy In-depth Report: Soil Contamination: Impacts on Human Health. Report produced for the European Commission DG Environment, http://ec.europa.eu/environment/integration/research/newsalert/pdf/IR5.pdf., (accessed August 2014).

12. IATP (Institute for Agriculture and Trade Policy), Suppan S. 2013. Nanomaterials In Soil. Our Future Food Chain?, http://www.iatp.org/files/2013_04_23_Nanotech_SS.pdf (accessed June 2015).
13. D. K. Tiwari, N. Dasgupta-Schubert, L. M. Villasenor Cendejas, J. Villegas, L. Carreto Montoya and S. E. Borjas Garcia, *Appl. Nanosci.*, 2014, **4**, 577–91.
14. B. Pan and B. S. Xing, *Environ. Sci. Technol.*, 2008, **42**, 9005-13.
15. X. L. Wang, S. Tao and B. S. Xing, *Environ. Sci. Technol.*, 2009, **43**, 6214-19.
16. N. Senesi and E. Loffredo, in *Soil Physical Chemistry*, ed. D. L. Sparks, 2ndedn., CRC Press, Boca Raton FL, 1999, pp. 239–370.
17. F. J. Stevenson, in *Humus Chemistry: Genesis, Composition, Reactions*, 2nd edn., Wiley & Sons Inc., Canada, 1994.
18. B. Vigneault, A. Percot, M. Lafleur and P. G. C. Campbell, *Environ. Sci. Technol.*, 2000, **34**, 3907-13.
19. L. M. Ojwang and R. L. Cook, *Environ. Sci. Technol.*, 2013, **47**, 8280-7.
20. E. Giannakopoulos, M. Drosos and Y. Deligiannakis, *J. Colloid Interf. Sci.*, 2009, **336**, 59–66.
21. D. Ziech, R. Franco, A. Pappa, V. Malamou-Mitsi, S. Georgakila, A. G. Georgakilas and M. I. Panayiotidis, *Chem-Biol. Interact.*, 2010, **188**, 340-9.
22. S. Bonassi, R. El-Zein, C. Bolognesi and M. Fenech, *Mutagenesis*, 2011,**26**, 93-100.
23. OECD. Test No. 487: In Vitro Mammalian Cell Micronucleus Test, OECD Guidelines for the Testing of Chemicals, Section 4, OECD Publishing, 2014, DOI: 10.1787/9789264224438-en.
24. V. Georgakilas, A. Bourlinos, D. Gournis, T. Tsoufis, C. Trapalis, A. Mateo-Alonso and M. Prato, *J. Am. Chem. Soc.*, 2008, **130**,8733-40.

25. M. Kirsch-Volders, T. Sofuni, M. Aardema, S. Albertini, D. Eastmond, M. Fenech, M. Ishidate Jr., S. Kirchner, E. Lorge, T. Morita, H. Norppa, J. Surralles, A. Vanhauwaert and A. Wakata, *Mutat. Res.*, 2003, **540**, 153-63.
26. M. Fenech, W. P. Chang, M. Kirsch-Volders, N. Holland, S. Bonassi and E. Zeiger, *Mutat. Res.*, 2003, **534**,65-75.
27. P. Papapaulou, D. Vlastos, G. Stephanou and N. A. Demopoulos, *Fresen. Environ. Bull.*, 2001, **10**, 421–37.
28. K. Hashimoto, Y. Nakajima, S. Matsumura and F. Chatani, *Toxicol. In Vitro*, 2010, **24**, 208–16.
29. S. Ghosh, H. Mashayekhi, B. Pan, P. Bhowmik and B. Xing, *Langmuir*, 2008, **24**, 12385-91.
30. L. D. Tickanen, M. I. Tejedor-Tejedor and M. A. Anderson, *Langmuir*, 1991, **7**, 451-6.
31. M. B. Hay and S. C. B. Myneni, *Geochim. Cosmochim. Ac.*, 2007, **71**, 3518-32.
32. D. Lin and B. Xing, *Environ. Sci. Technol.*, 2008, **42**, 7254-9.
33. G. Clare, G. Lorenzon, L. Akhurst, D. Marzin, J. van Delft, R. Montero, A. Botta, A. Bertens, S. Cinelli, V. Thybaud and E. Lorge, *Mutat Res*., 2006, **607**, 37-60.
34. D. Vlastos, C. G. Skoutelis, I. T. Theodoridis, D. R. Stapleton and M. I. Papadaki, *J. Hazard. Mater.*, 2010, **177**, 892–8.
35. C. G. Skoutelis, D. Vlastos, M. C. Kortsinidou, I. T. Theodoridis and M. I. Papadaki, *J. Hazard. Mater.*, 2011, **197**, 137–43.
36. E. Toufexi, V. Tsarpali, I. Efthimiou, M-S. Vidali, D. Vlastos and S. Dailianis, *J. Hazard. Mater.*, 2013, **260**, 593-601.
37. L. Gonzalez, B. J. S. Sanderson and M. Kirsch-Volders, *Mutagenesis*, 2011, **26**, 185–91.
38. H. K. Lindberg, G. C. M. Falck, S. Suhonen, M. Vippola, E. Vanhala, J. Catalán, K. Savolainen and H. Norppa, *Toxicol. Lett.*, 2009, **186**, 166-73.

39. M. Ghosh, A. Chakraborty, M. Bandyopadhyay and A. Mukherjee, *J. Hazard. Mater.*, 2011, **197,** 327-36.
40. A.M. Tavares, H. Louro, S. Antunes, S. Quarré, S. Simar, P.-J. De Temmerman, E. Verleysen, J. Mast, K.A. Jensen, H. Norppa, F. Nesslany and M.J. Silva, *Toxicol in Vitro*, 2014, **28**, 60-9.
41. G. Ferrara, E. Loffredo, N. Senesi and R. Marcos, *Mutat. Res.*, 2006, **603**, 27–32.
42. J. Cveticanin, G. Joksic, A. Leskovac, S. Petrovic, A. V. Sobot and O. Neskovic, *Nanotechnology*, 2010, DOI:10.1088/0957-4484/21/1/015102.
43. I. Muller, I. Decordier, P. Hoet, N. Lombaert, I. Thomassen, F. Huaux, D. Lison and M. Kirsch-Volders, *Carcinogenesis*, 2008, **29**, 427-33.
44. Y. Kihara, Yustiawati, M. Tanaka, S. Gumiri, Ardianor, T. Hosokawa, S. Tanaka, T. Saito and M. Kurasaki, *Environ. Toxicol.*, 2014, **29**, 916–25.
45. L. Lacerda, A. Soundararajan, R. Singh, G. Pastorin, K. T. Al-Jamal, J. Turton, P. Frederik, M. A. Herrero, S. L. A. Bao, D. Emfietzoglou, S. Mather, W. T. Phillips, M. Prato, A. Bianco, B. Goins and K. Kostarelos, *Adv. Mater.*, 2008, **20**, 225–30.
46. X. Deng, G. Jia, H. Wang, H. Sun, X. Wang, S. Yang, T. Wang and Y. Liu, *Carbon*, 2007, **45**, 1419–424.
47. M. Pacurari, Y. Qian, W. Fu, D. Schwegler-Berry, M. Ding, V. Castranova and N. L. Guo, *J. Toxicol. Environ. Health A*, 2012, **75**, 112–28.
48. J. H. Shannahan, J. M. Brown, R. Chen, P. C. Ke, X. Lai, S. Mitra and F. A. Witzmann, *Small*, 2013, **9**, 2171-81.
49. L. Gonzalez, M. Lukamowicz-Rajska, L. C. J. Thomassen, C. E. A. Kirschhock, L. Leyns, D. Lison, J. A. Martens, A. Elhajouiji and M. Kirsch-Volders, *Nanotoxicology*, 2014, **8**, 876–84.

50. V. Raffa, L. Gherardini, O. Vittorio, G. Bardi, A. Ziaei, T. Pizzorusso, C. Riggio, S. Nitodas, T. Karachalios, K. T. Al-Jamal, K. Kostarelos, M. Costa and A. Cuschieri, *Nanomedicine(Lond)*, 2011, **6**, 1709-18.

Table Legends

Table 1.Frequencies of MN as well as CBPI values in cultured human lymphocytes treated with MWCNTs, LHA and their mixture.

Table 2. Frequencies of MN as well as CBPI values in cultured human lymphocytes treated with MWCNTs, HALP and their mixture.

Figure Legends

Figure 1. (a) Formation of a stable water-dispersible form of CNTs in the absence of HALP (50 ppm CNTs in H_2O pH 7), (b) 50 ppm HALP pH 7 (c) 50 ppm CNTs in H_2O plus 50 ppm HALP pH 7 (30 min bath-sonication, the dispersion shown remained unaltered after six days). (d) Same as (c) after 120 min bath-sonication. (e) 50 ppm CNTs in H_2O plus 50 ppm LHA pH 7, 120 min bath-sonication.

Figure 2. Dynamic Light Scattering number-distributions of MWCNTs (a) in H_2O and (b) in cell-culture medium. (Blue lines): MWCNTs, (Red lines): MWCNTs+HALP. The suspensions were sonicated with a total energy 0.6 kJ/ml and measured within 30 minutes after sonication. The black trace in (b) is for the MWCNTs+HALP sample left for 72hours at rest.

Figure 3. (a) ATR-FTIR spectra of HALP (black line) 50ppm and CNTs-HALP (red line) 50 ppm at pH 5.0 (i), 6.5 (ii) or 8.5 (iii) and (b) ATR-FTIR spectra of LHA (black line) 50 pm and CNTs-LHA (red line) 50 ppm at pH 5.0 (i), 6.5 (ii) or 8.5 (iii).

Figure 4. AFM images and section analysis of (a) pure MWCNTs and (b) MWCNTs-HALP at pH 4.0. (a) MWCNTs in the absence of HA shows the aggregated structure of MWCNTs, (b) MWCNTs obtain a mono-disperse structure after interaction with the HAs.

Table 1.

Frequencies of MN as well as CBPI values in cultured human lymphocytes treated with MWCNTs, LHA and their mixture.

Concentration (µg/ml)	MN MF(‰)±se	CBPI MF(‰)±se
0	5.25±0.48	1.78±0.02
MWCNTs		
5	12.25±1.44**	1.78±0.01
15	10.75±0.63*	1.77±0.02
25	9.00±0.41	1.77±0.02
LHA		
20	8.50±0.50	1.79±0.01
60	9.75±0.85	1.77±0.02
100	9.50±0.29	1.80±0.01
MWCNTs+LHA		
5+20	20.25±0.25***	1.76±0.04
15+ 60	18.50±0.96***	1.75±0.05
25+100	24.00±1.78***	1.75±0.03
MMC		
0.05	54.75±4.13***	1.67±0.02**

MN, micronuclei; CBPI, Cytokinesis Block Proliferation Index; MF(‰)±se, mean frequencies (‰)±standard error; MWCNTs, multi-walled carbon nanotubes; LHA, Leonardite humic acid; MMC, Mitomycin-C; 4000 binucleated cells scored per experimental point; *p<0.05, **p<0.01, ***p<0.001 [G-test for MN; χ^2 for CBPI]

Table 2.

Frequencies of MN as well as CBPI values in cultured human lymphocytes treated with MWCNTs, HALP and their mixture.

Concentration (µg/ml)	MN MF(‰)±se	CBPI MF(‰)±se
0	5.0±0.0	1.84±0.01
MWCNTs		
5	9.5±0.5	1.84±0.01
15	9.5±0.5	1.83±0.04
25	8.5±0.5	1.83±0.01
30	8.5±0.5	1.84±0.01
HALP		
8	5.0±0.0	1.83±0.01
25	5.5±0.5	1.90±0.06
42	6.5±0.5	1.86±0.02
50	6.5±0.5	1.84±0.03
MWCNTs+HALP		
5+8	13.5±0.5*	1.84±0.02
15+25	14.5±0.5**	1.86±0.03
25+42	15.0±1.0**	1.88±0.02
30+50	17.0±0.0**	1.90±0.01
MMC		
0.05	57.0±6.0**	1.67±0.02**

MN, micronuclei; CBPI, Cytokinesis Block Proliferation Index; MF(‰)±se, mean frequencies (‰)±standard error; MWCNTs, multi-walled carbon nanotubes; HALP, Humic-acid-like polycondensates; MMC, Mitomycin-C; 2000 binucleated cells scored per experimental point; *p<0.01, **p<0.001 [G-test for MN; $\chi^2$for CBPI]

671

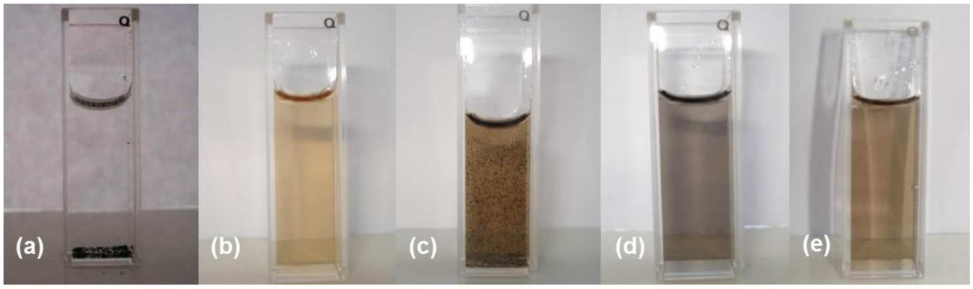

Figure 1. (a) Formation of a stable water-dispersible form of CNTs in the absence of HALP (50 ppm CNTs in H2O pH 7), (b) 50 ppm HALP pH 7 (c) 50 ppm CNTs in H2O plus 50 ppm HALP pH 7 (30 min bath-sonication, the dispersion shown remained unaltered after six days). (d) Same as (c) after 120 min bath-sonication. (e) 50 ppm CNTs in H2O plus 50 ppm LHA pH 7, 120 min bath-sonication.
190x142mm (300 x 300 DPI)

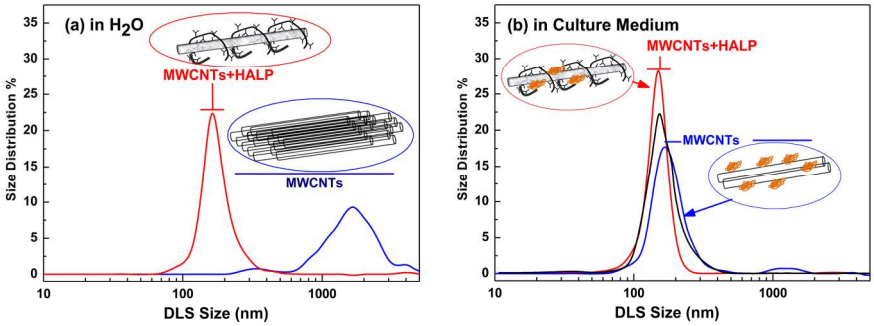

Figure 2. Dynamic Light Scattering number-distributions of MWCNTs (a) in H2O and (b) in cell-culture medium. (Blue lines): MWCNTs, (Red lines): MWCNTs+HALP. The suspensions were sonicated with a total energy 0.6 kJ/ml and measured within 30 minutes after sonication. The black trace in (b) is for the MWCNTs+HALP sample left for 72hours at rest.
190x142mm (300 x 300 DPI)

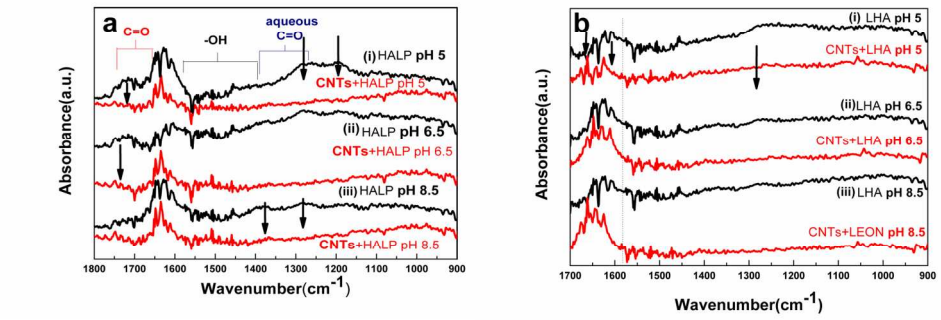

Figure 3. (a) ATR-FTIR spectra of HALP (black line) 50ppm and CNTs-HALP (red line) 50 ppm at pH 5.0 (i), 6.5 (ii) or 8.5 (iii) and (b) ATR-FTIR spectra of LHA (black line) 50 pm and CNTs-LHA (red line) 50 ppm at pH 5.0 (i), 6.5 (ii) or 8.5 (iii).
190x142mm (300 x 300 DPI)

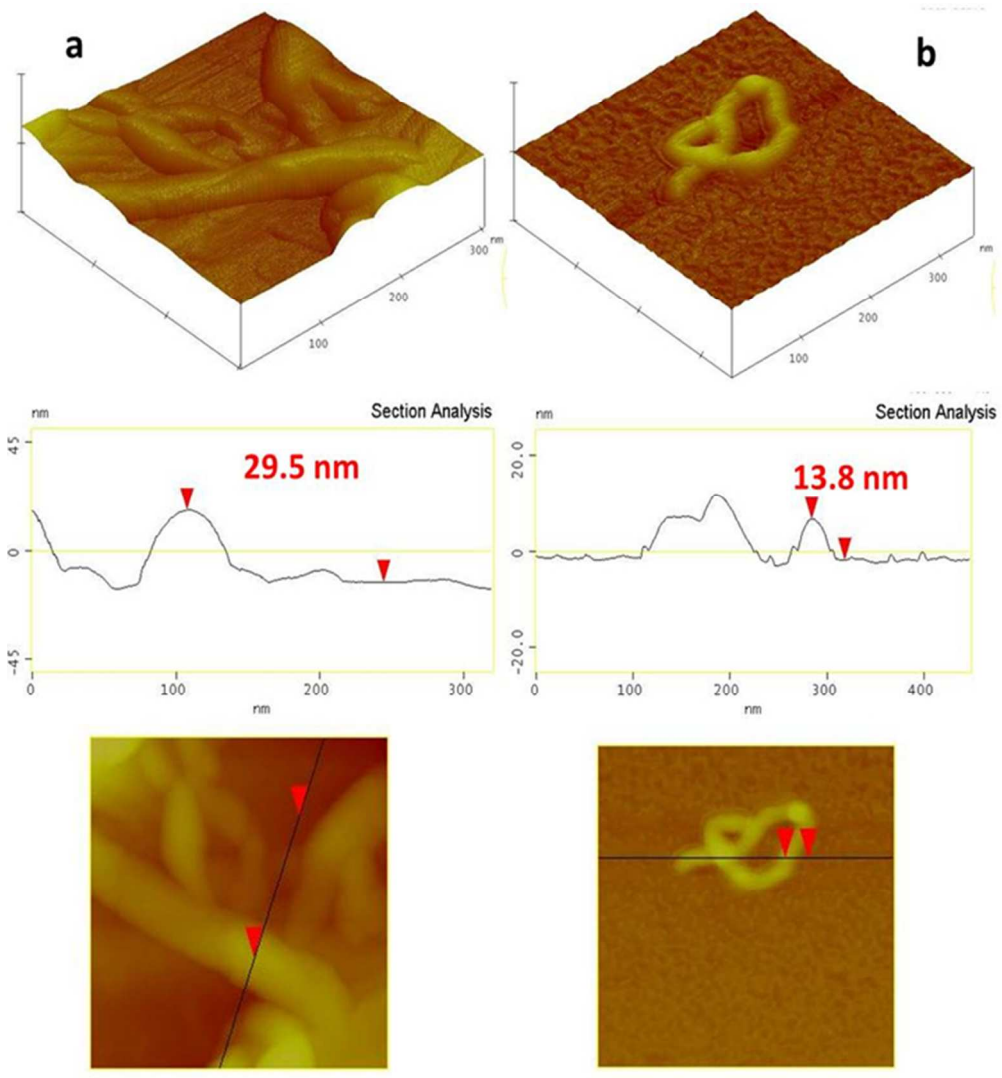

Figure 4. AFM images and section analysis of (a) pure MWCNTs and (b) MWCNTs-HALP at pH 4.0. (a) MWCNTs in the absence of HA shows the aggregated structure of MWCNTs, (b) MWCNTs obtain a mono-disperse structure after interaction with the HAs.
121x131mm (150 x 150 DPI)